



Liquid-phase synthesis of Li₃PS₄ solid electrolyte using ethylenediamine

メタデータ	言語: English 出版者: Springer Nature 公開日: 2024-07-17 キーワード (Ja): キーワード (En): All-solid-state lithium battery, Solid electrolyte, Liquid-phase synthesis, Sulfide, Lithium-ion conductivity 作成者: Ito, Akane, Kimura, Takuya, 作田, 敦, 辰巳砂, 昌弘, 林, 晃敏 メールアドレス: 所属:
URL	http://hdl.handle.net/10466/0002001024

Liquid-phase synthesis of Li_3PS_4 solid electrolyte using ethylenediamine

Akane Ito^a, Takuya Kimura^a, Atsushi Sakuda^{a,*}, Masahiro Tatsumisago^a, Akitoshi Hayashi^{a,**}

a) Department of Applied Chemistry, Graduate School of Engineering, Osaka Prefecture University, 1-1, Gakuen-cho, Naka-ku, Sakai, Osaka 599-8531, Japan

*, ** Corresponding Author

Email: *saku@chem.osakafu-u.ac.jp

**hayashi@chem.osakafu-u.ac.jp

Highlights:

- $\beta\text{-Li}_3\text{PS}_4$ is prepared via liquid-phase synthesis using a ethylenediamine solution.
- Ethylenediamine effectively suppresses the decomposition of PS_4^{3-} .
- The ionic conductivity of the prepared $\beta\text{-Li}_3\text{PS}_4$ is $5 \times 10^{-5} \text{ S cm}^{-1}$ at 25 °C.

Abstract

Li_3PS_4 is the most typical solid electrolytes for all-solid-state lithium batteries. However, to date, there are few reports on Li_3PS_4 solid electrolyte synthesized using the solution process. Here, $\beta\text{-Li}_3\text{PS}_4$ solid electrolytes were prepared via liquid-phase synthesis by dissolving Li_2S and P_2S_5 in ethylenediamine (EDA) to form a homogeneous solution of Li_3PS_4 . Since EDA is a basic protonic solvent, it effectively suppressed the decomposition of Li_3PS_4 . An intermediate phase consisting of Li_3PS_4 and EDA was formed as a precursor after drying the EDA solution at 200 °C under vacuum. After heat treatment at temperatures above 260 °C, $\beta\text{-Li}_3\text{PS}_4$ was crystallized from the precursor. The ionic conductivity of the prepared $\beta\text{-Li}_3\text{PS}_4$ was $5.0 \times 10^{-5} \text{ S cm}^{-1}$ at 25 °C and the activation energy for conduction was 35 kJ mol⁻¹. The obtained EDA solution of Li_3PS_4 will be effective in forming electrolyte-electrode interfaces with the large contact areas in all-solid-state batteries.

Keywords

All-solid-state lithium battery, Solid electrolyte, Liquid-phase synthesis, Sulfide, Lithium ion conductivity

Declarations

Funding

This work was partially supported by JST ALCA-SPRING (Grant JPMJAL1301), Japan.

Conflicts of interest/Competing interests

The authors declare that they have no conflict of interest.

1. Introduction

Lithium-ion batteries (LIBs) are extensively used as power sources for various electronic devices owing to their high energy densities [1]. However, due to the use of organic liquid electrolytes, LIBs suffer from the associated safety issues. Solid-state batteries using nonflammable inorganic solid electrolytes (SEs) can mitigate this risk and are can be installed in electric and hybrid vehicles to improve their safety. Recently, sulfide-based SEs, with high Li-ion conductivities and favorable mechanical properties, have been investigated as promising electrolyte materials. In 2011, Kanno *et al.* reported that $\text{Li}_{10}\text{GeP}_2\text{S}_{12}$ crystals showed a high Li-ion conductivity of $1.2 \times 10^{-2} \text{ S cm}^{-1}$ at 25 °C [2]. Furthermore, in 2016, they reported that $\text{Li}_{9.54}\text{Si}_{1.74}\text{P}_{1.44}\text{S}_{11.7}\text{Cl}_{0.3}$ exhibited an extremely high conductivity of $2.5 \times 10^{-2} \text{ S cm}^{-1}$ [3]. In addition, the crystalline phases and the Li-ion conductivities of binary $\text{Li}_2\text{S}-\text{P}_2\text{S}_5$ systems have been studied. In 2014, we reported that $70\text{Li}_2\text{S}\cdot 30\text{P}_2\text{S}_5$ glass-ceramic, which was first reported in 2005 [4], exhibited a high Li-ion conductivity of $1.7 \times 10^{-2} \text{ S cm}^{-1}$ at 25 °C. The conductivities are

comparable to those of the organic liquid electrolytes used in LIBs.

SEs have been synthesized mainly by mechanochemical processes, melt quenching, and solid-state reactions. Recently, the liquid-phase synthesis of SEs has attracted attention for their mass production. In the liquid-phase synthesis, the starting materials are dispersed in liquid as a reaction medium and the resulting suspension or solution is dried and heat-treated to obtain the SE. The synthesis process can be categorized into two types of processes: suspension process and solution one [5].

Suspension synthesis is conducted by stirring the starting materials in aprotic solvents, such as ethers and nitriles. In 2013, the suspension syntheses of Li_3PS_4 have reported using tetrahydrofuran (THF) [6]. Subsequently, the suspension synthesis of Li_3PS_4 have reported using various solvents such as acetonitrile (ACN) [7], ethyl acetate [8], ethyl propionate [9], and dibutyl ether [10]. It is noteworthy that $\text{Li}_7\text{P}_3\text{S}_{11}$ [11] and $\text{Li}_7\text{P}_2\text{S}_8\text{I}$ [12] with high conductivities were prepared using ACN.

On the other hand, solution synthesis is conducted by dissolving the starting materials in protic solvents, such as alcohols and water. The SEs are obtained relatively quicker in the solution process than in the suspension process. Moreover, the resulting homogeneous solution is effective in forming composite electrodes with intimate electrode-electrolyte interfaces. To date, there are very few reports on SEs synthesized

using the solution process. Wang *et al.* have reported that $\text{Li}_{3.25}\text{Ge}_{0.25}\text{P}_{0.75}\text{S}_4$ is synthesized by dissolving the SE prepared by solid-state reactions into hydrazine to form homogenous solution and drying [13]. Young Eun Choi *et al.* have reported that Li_4SnS_4 SE is synthesized using deionized water [14]. We have reported that $\text{Li}_6\text{PS}_5\text{Br}$ is synthesized from the mixture of Li_2S , P_2S_5 and LiBr by solution processes using THF and ethanol [15]. In our previous paper, we had reported on a Li_3PS_4 SE that was prepared by a solution process using N-methylformamide (NMF) [16]. The ionic conductivity of the SE was $2.6 \times 10^{-6} \text{ S cm}^{-1}$ at 25 °C, which is lower than that of the mechanochemically prepared Li_3PS_4 with the conductivity of $10^{-4} \text{ S cm}^{-1}$ [17]. This low conductivity is presumably due to the residual starting materials, partial decomposition of the phosphorus sulfide units as PS_4^{3-} , and solvent residue. To synthesize Li_3PS_4 with high ionic conductivity by a solution process, it is important to propose synthesis conditions that suppress such deterioration factors.

Ethanol, a protic solvent, is frequently used as the solvent for synthesizing SEs via the solution process. Unfortunately, it is difficult to prepare Li_3PS_4 using ethanol because the hydroxyl groups decompose the P–S–P bonds in the starting material, P_2S_5 [14, 18]. In this study, ethylenediamine (EDA), which is a protic solvent with a suitable boiling point (<150 °C), was selected as the dispersion medium, and Li_3PS_4 was synthesized via

the solution process. EDA does not contain hydroxyl groups or oxygen, and hence, we hypothesized that the decomposition of the phosphorus sulfide units and contamination of the oxides would be suppressed, thus increasing the ionic conductivity of the product. The structures of the precursor and final products prepared from the EDA solution were analyzed and the conductivities of the resulting β -Li₃PS₄ SEs were examined.

2. Experimental

A Li₃PS₄ SE was synthesized via a liquid-phase reaction using EDA (Wako, 99.0 %) as the solvent and Li₂S (Mitsuwa, 99.9 %) and P₂S₅ (Aldrich, 99 %) as the starting materials. The Li₂S and P₂S₅ with a molar ratio of 3:1 were dissolved in 18 g of EDA and stirred at 25 °C for 3 h. In this study, the SEs were prepared with the theoretical composition of Li₃PS₄ on the premise that the obtained solution or the whole amount of powder was used. The total weight of the starting material was 1 g. The concentration of EDA solution of the mixture corresponded to *ca.* 5 wt.%. After stirring, the obtained solution was dried at 200 °C to prepare the Li₃PS₄ precursor. The drying was conducted under reduced pressure to obtain the Li₃PS₄ precursor in a short time and at low temperature to avoid unfavorable side reactions. The precursor was then heat-treated in a dry Ar atmosphere at 260 and 330 °C, as determined by thermogravimetric and

differential thermal analysis (TG-DTA). TG-DTA was performed using a thermal analyzer (Thermo-plus 8110, Rigaku Co.) in the temperature range from 20 to 550 °C at heating rate of 10 °C min⁻¹ under N₂ gas flow. The structural units in the EDA solution and the powders obtained after drying and heat treatment were identified using a Raman spectrophotometer (LabRAM HR-800, HORIBA Ltd.) equipped with a 532-nm solid-state laser. X-ray diffraction (XRD) measurements were conducted using an X-ray diffractometer (SmartLab, Rigaku) with Cu-K α radiation. Diffraction data were collected over a 2θ range 5–80° in steps of 0.02° at a scan rate of 10° min⁻¹. The XRD measurements were performed using an airtight container with a Be window, to prevent exposure to air.

To investigate the stability of Li₃PS₄ in solvent, a Li₃PS₄ glass was synthesized by a mechanochemical (MC) technique. The MC treatment was carried out using a planetary ball mill (Pulverisette 5, Fritsch) with a zirconia pot (250 mL in volume) and zirconia balls (4 mm in diameter, 450 g) at ambient temperature. The rotational speed was set at 210 rpm and the milling time was 50 h.

The ionic conductivity of the β -Li₃PS₄ obtained from the EDA solution was measured by measuring the AC impedance, using an impedance analyzer (Solartron, 1260) in the frequency range from 1 Hz to 1 MHz. The measurement was performed on a pellet which

was 10 mm in diameter and approximately 1.0 mm thick that was prepared by cold-pressing at 360 MPa. Au current collectors were used to cover the entire surface on both sides of the pellet. All the measurements were performed in a dry Ar atmosphere.

3. Results and discussion

First, a Li_3PS_4 glass prepared via a MC process was dissolved in EDA, and the structural change of the material in the solution was tracked to investigate the stability of Li_3PS_4 in EDA. For comparison, the same operation was performed using an ethanol solution. Figure 1 shows the Raman spectra of the EDA solution of the Li_3PS_4 glass, stirred for different durations, and Figure 2 shows the spectra of the ethanol solution for comparison. When ethanol is used, the peak at approximately 420 cm^{-1} , attributable to the PS_4^{3-} unit [14], is not observed in the Raman spectrum after 10 min of stirring. The band centered at 380 and 480 cm^{-1} observed in the Raman spectrum of an ethanol solution are attributed to Li_2S and the S-S bonds [19], respectively, suggesting that Li_3PS_4 decompose in ethanol. However, the peak for PS_4^{3-} unit is observed in the Raman spectrum of the EDA solution even after 3 days of stirring, suggesting that the PS_4^{3-} unit is much more stable in EDA than in ethanol. The intensity of peak for PS_4^{3-} unit in the Raman spectrum of the EDA solution after stirring for 3 h is the highest in the Raman

spectra of the EDA solution studied here. The stirring time of 3 h was thus chosen for synthesis of Li_3PS_4 .

Li_3PS_4 was synthesized from Li_2S and P_2S_5 using EDA as the solvent. TG-DTA measurements were performed to determine the heat-treatment temperatures of the sample dried at 200 °C. As shown in Figure 3, the TG curve shows a weight loss at approximately 250 °C, which is due to the desorption of the solvent. A large endothermic peak near 290°C is observed in the DTA curve, therefore, the heat treatment process was performed at the temperatures before and after the weight loss (200 and 260 °C) and after the exothermic peak at 330 °C.

Figure 4 shows the XRD patterns of the powders obtained from the precursor solution after drying at 200 °C under vacuum (precursor) and after heat treatment (HT) at 260, and 330 °C. In the XRD pattern of the precursor powder, diffraction peaks attributable to a new phase are observed. The XRD patterns of the samples after heat treatment of the precursor are mainly attributable to $\beta\text{-Li}_3\text{PS}_4$. The low-intensity peak near $2\theta = 27^\circ$ is due to the Li_2S phase, indicating that unreacted Li_2S remains partially. In addition, the XRD pattern of the powder obtained after heat treatment at 330 °C has unknown peaks with low intensity, suggesting the presence of impurities.

Figure 5 shows the Raman spectra of the powders obtained from the solution after

drying at 200 °C under vacuum (precursor) and after heat treatment at 260 and 330 °C. The main band at 420 cm⁻¹ corresponding to the PS₄³⁻ unit of the Li₃PS₄ is clearly observed in the Raman spectra of all the samples. It is noted that the precursor has PS₄³⁻ as a thio-phosphate unit and is expected to be a solvated salt consisting of Li⁺, PS₄³⁻, and EDA.

Figure 6 shows the temperature dependence of the conductivities of the SEs obtained by heat treatment of the precursor at 260 and 330 °C in a dry Ar atmosphere. For the samples heat-treated at 260 °C, the conductivities are found to be 5.0×10^{-5} S cm⁻¹ at 25 °C. This value is more than 10 times higher than that of the Li₃PS₄ SE synthesized from an NMF solution [16]. These conductivities obey the Arrhenius law and the activation energy for conduction that is calculated from the slope of the plots is 35 kJ mol⁻¹. The conductivity at 25 °C of the sample heat-treated at 330 °C is 4.3×10^{-5} S cm⁻¹, which is slightly lower than the conductivity of the sample that was heat-treated at 260 °C. The slight decrease in conductivity after heat treatment at 330 °C is likely caused by the presence of impurity phases, as shown in Figure 4.

4. Conclusion

In this study, EDA was used for the first time as the solvent for the liquid-phase

synthesis of Li_3PS_4 from Li_2S and P_2S_5 . The improved stability of PS_4^{3-} in EDA compared to that in ethanol was confirmed. The $\beta\text{-Li}_3\text{PS}_4$ phase was prepared after heat-treatment of the dried precursor powders at 260 °C. The ionic conductivity of the prepared SE was $5.0 \times 10^{-5} \text{ S cm}^{-1}$ at 25 °C and the activation energy for conduction was 35 kJ mol⁻¹. Liquid-phase synthesis with EDA is thus a simple way to synthesize sulfide-based SEs with superior conductivity by suppressing the side reactions.

References

1. Tarascon JM, Armand M (2001) Nature 414:359–367.
<https://doi.org/10.1038/35104644>
2. Kamaya N, Homma K, Yamakawa Y, Hirayama M, Kanno R, Yonemura M, Kamiyama T, Kato Y, Hama S, Kawamoto K, Mitsui A (2011) Nat Mater 10:682–686.
<https://doi.org/10.1038/nmat3066>
3. Kato Y, Hori S, Saito T, Suzuki K, Hirayama M, Mitsui A, Yonemura M, Iba H, Kanno R (2016) Nat Energy 1:16030. <https://doi.org/10.1038/nenergy.2016.30>
4. Mizuno F, Hayashi A, Tadanaga K, Tatsumisago M (2005) Adv Mater 17:918–921. <https://doi.org/10.1002/adma.200401286>
5. Miura A, Rosero-Navarro N C, Sakuda A, Tadanaga K, Phuc N H H, Matsuda

- A, Machida N, Hayashi A, Tatsumisago M (2021) *J Mater Chem A* 9: 400–405.
<https://doi.org/10.1039/D0TA08658D>
6. Liu Z, Fu W, Payzant EA, Yu X, Wu Z, Dudney NJ, Kiggans J, Hong K, Rondinone AJ, Liang C (2013) *J Am Chem Soc* 135:975–978.
<https://doi.org/10.1021/ja3110895>
7. Wang H, Hood Z D, Xia Y, Liang C (2016) *J Mater Chem A* 4:8091–8096.
<https://doi.org/10.1039/C6TA02294D>
8. Phuc N H H, Totani M, Morikawa K, Muto H, Matsuda A (2016) *Solid State Ionics* 288:240–243. <https://doi.org/10.1016/j.ssi.2015.11.032>
9. Phuc N H H, Morikawa K, Mitsuhiro T, Muto H, Matsuda A (2017) *Ionics* 23:2061–2067. <https://doi.org/10.1007/s11581-017-2035-8>
10. Choi S, Lee S, Park J, Nichols WT, Shin D (2018) *Appl Surface Sci* 444:10–14.
<https://doi.org/10.1039/C6TA10142A>
11. Xu RC, Wang XL, Zhang SZ, Xia Y, Xia XH, Wu JB, Tu JP (2018) *J Power Sources* 374:107–112. <https://doi.org/10.1016/j.jpowsour.2017.10.093>
12. Rangasamy E, Liu Z, Gobet M, Pilar K, Sahu G, Zhou W, Wu H, Greenbaum S, Liang C (2015) *J Am Chem Soc* 137:1384–1387. <https://doi.org/10.1021/ja508723m>
13. Wang Y, Liu Z, Zhu X, Tang Y, Huang F (2013) *J Power Sources* 224:225–229.

<https://doi.org/10.1016/j.jpowsour.2012.09.097>

14. Choi YE, Park KH, Kim DH, Oh DY, Kwak HR, Lee Y-G, Jung YS (2017) ChemSusChem 10:2605–2611. <https://doi.org/10.1002/cssc.201700409>
15. Yubuchi S, Uematsu M, Hotehama C, Sakuda A, Hayashi A, Tatsumisago M (2019) J Mater Chem A 7:558–566. <https://doi.org/10.1039/C8TA09477B>
16. Teragawa S, Aso K, Tadanaga K, Hayashi A, Tatsumisago M (2014) J Power Sources 248:939–942. <https://doi.org/10.1016/j.jpowsour.2013.09.117>
17. Hayashi A, Hama S, Morimoto H, Tatsumisago M, Minami T (2001) J Am Ceram Soc 84:477–79. <https://doi.org/10.1111/j.1151-2916.2001.tb00685.x>
18. Ozturk T, Ertas E, Mert O (2010) Chem Rev 110:3419–3478. <https://doi.org/10.1021/cr900243d>
19. Mizuno F, Hayashi A, Tadanaga K, Tatsumisago M (2005) Solid State Ionics 176:2349–2353. <https://doi.org/10.1016/j.ssi.2005.03.025>

Figure. 1 Raman spectra of the supernatant EDA solution with Li_3PS_4 glass after stirring for different periods of time.

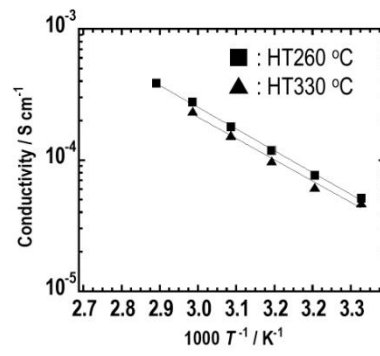
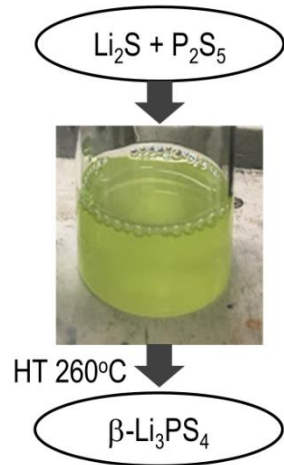
Figure. 2 Raman spectra of the supernatant ethanol (EtOH) solution with Li_3PS_4 glass after stirring for different periods of time.

Figure. 3 TG-DTA curves of the Li_3PS_4 samples synthesized using EDA and dried at 200 °C.

Figure. 4 XRD patterns of the Li_3PS_4 SEs synthesized from the mixture of Li_2S and P_2S_5 using EDA.

Figure. 5 Raman spectra of the Li_3PS_4 SEs synthesized using EDA.

Figure. 6 Temperature dependence of the conductivities of the Li_3PS_4 SEs synthesized using EDA.



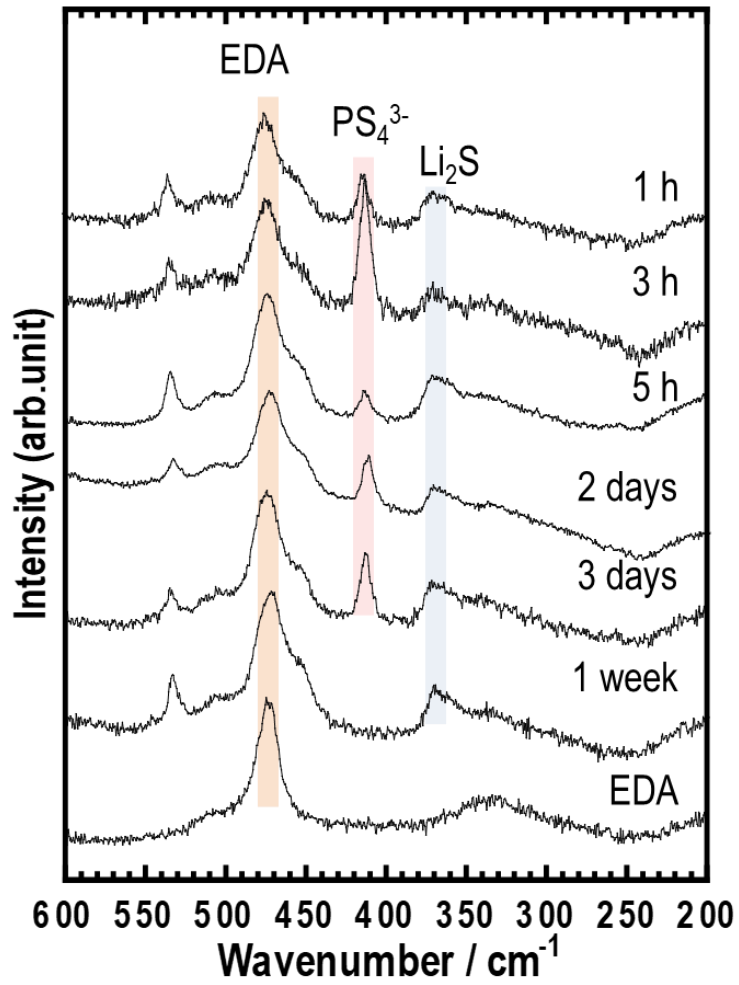


Fig. 1 Raman spectra of the supernatant EDA solution with Li_3PS_4 glass after stirring for different periods of time.

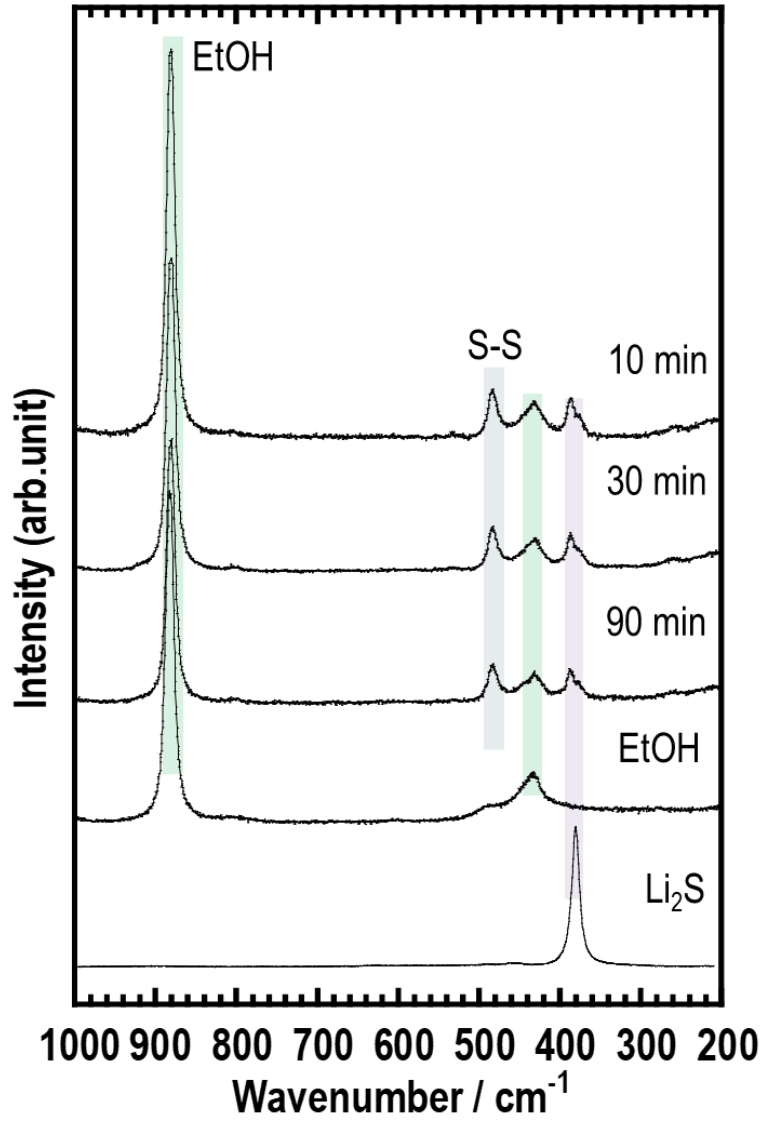


Fig. 2 Raman spectra of the supernatant ethanol (EtOH) solution with Li₃PS₄ glass after stirring for different periods of time.

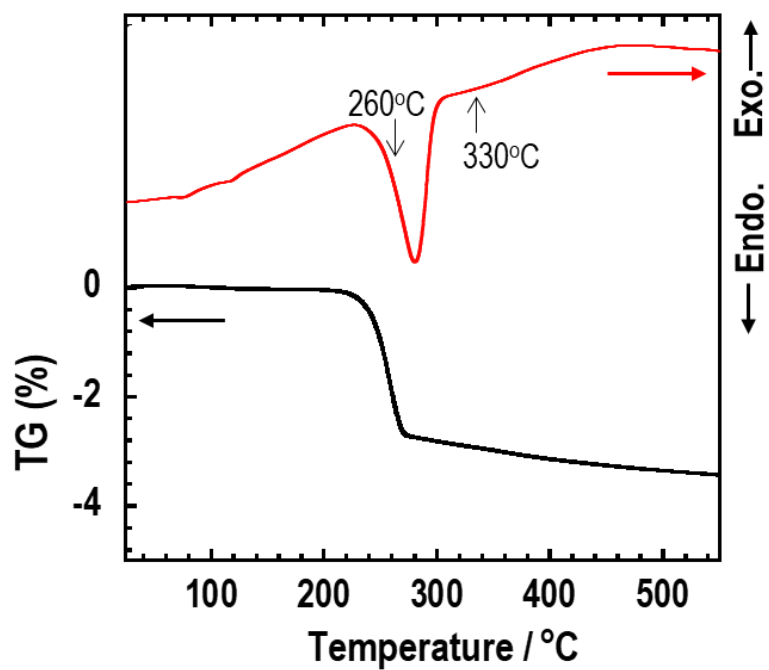


Fig. 3 TG-DTA curves of the Li_3PS_4 samples synthesized using EDA and dried at 200 °C.

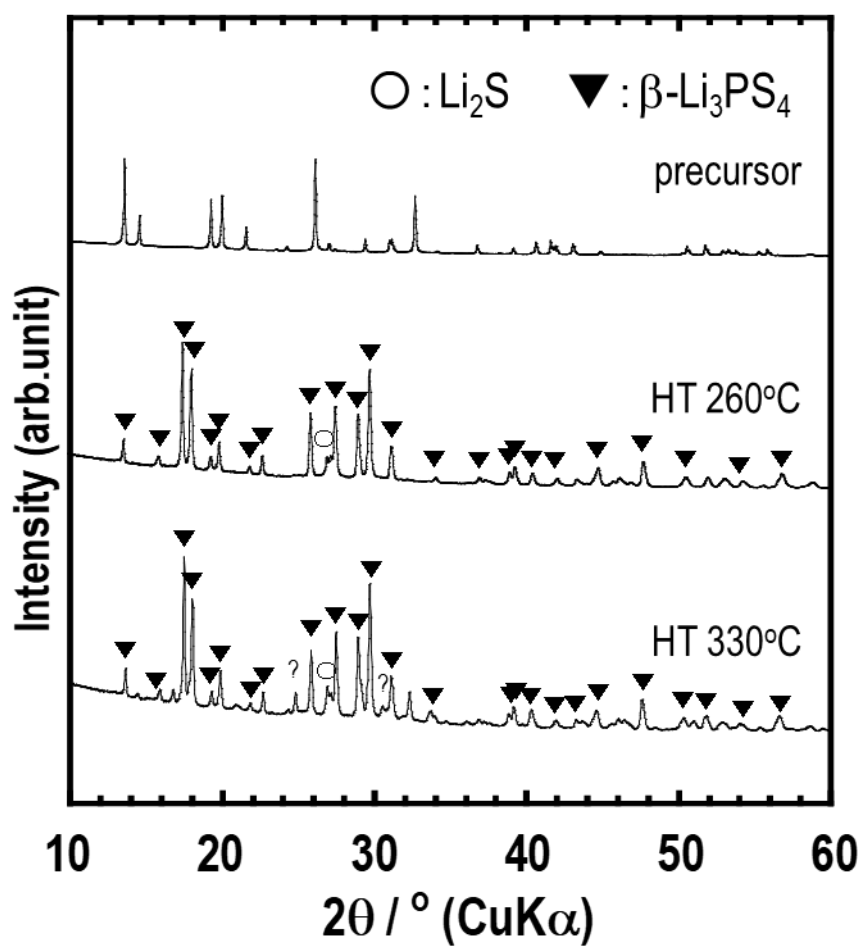


Fig. 4 XRD patterns of the Li_3PS_4 SEs synthesized from the mixture of Li_2S and P_2S_5 using EDA.

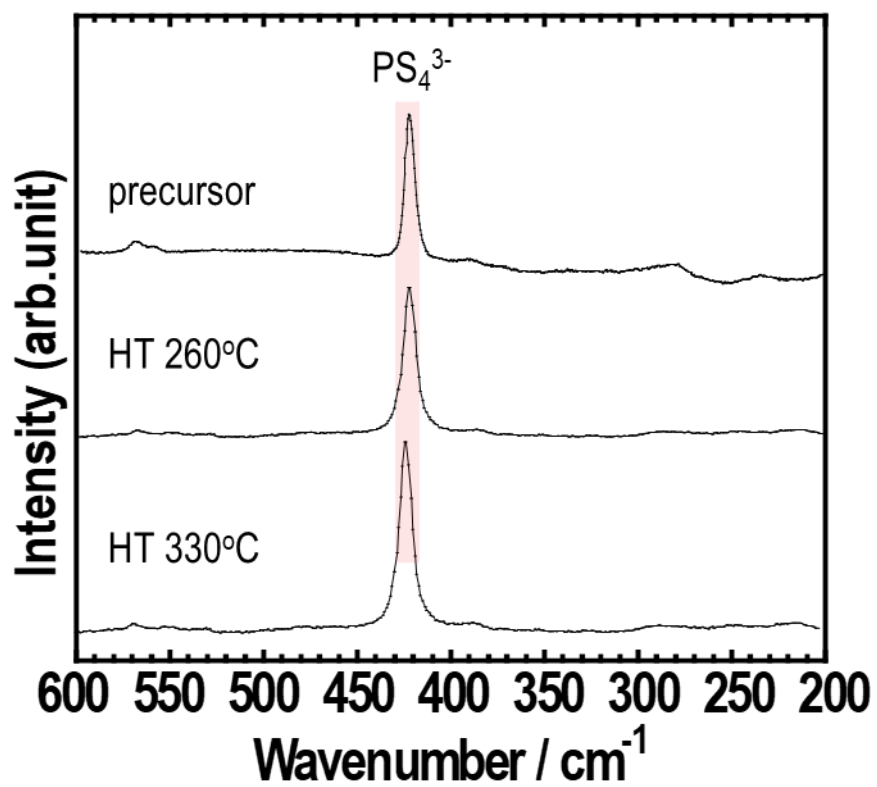


Fig. 5 Raman spectra of the Li_3PS_4 SEs synthesized using EDA.

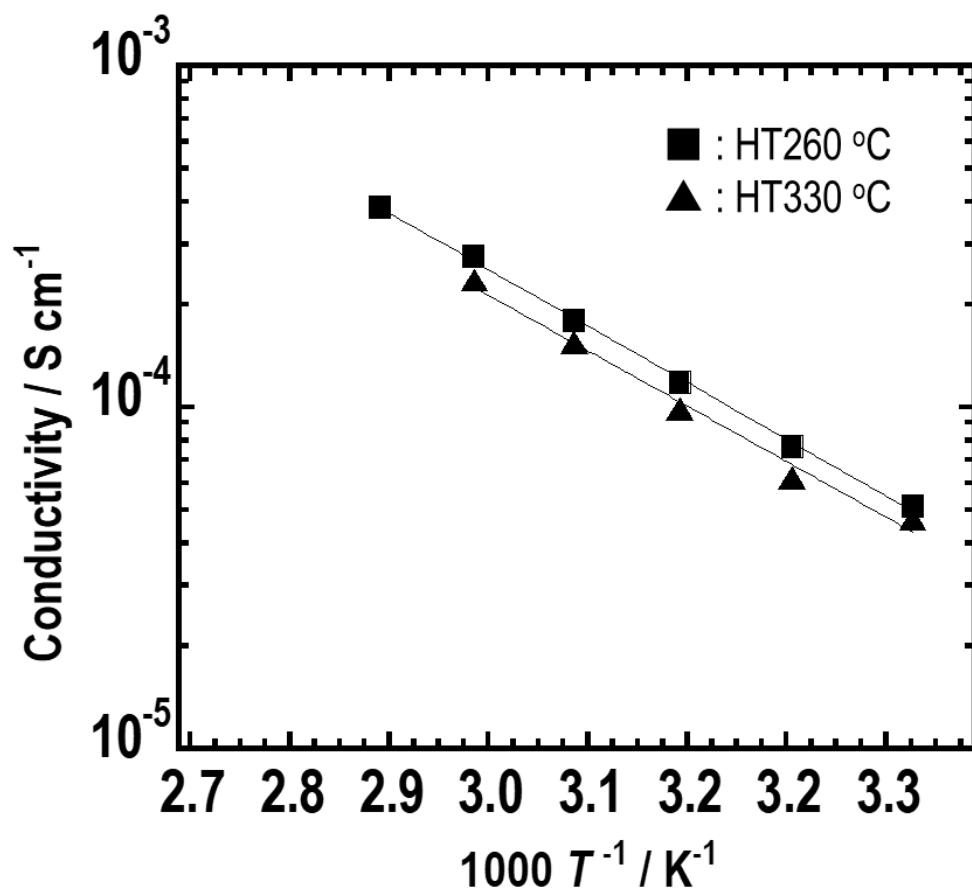


Fig. 6 Temperature dependence of the conductivities of the Li_3PS_4 SEs synthesized using EDA.